

¹ **The Hawaiian Educational Radar Opportunity (HERO)**

² MICHAEL M. BELL^{1*}, ROBERT A. BALLARD^{1,2}, MARK BAUMAN¹,
ANNETTE M. FOERSTER¹, ANDREW FRAMBACH¹, KAREN A. KOSIBA⁴,
WEN-CHAU LEE³, SHANNON L. REES^{1†}, AND JOSHUA WURMAN⁴

¹ *University of Hawai‘i at Mānoa, Honolulu, Hawai‘i*

² *National Weather Service, Honolulu, Hawai‘i*

³ *National Center for Atmospheric Research, Boulder, Colorado*

⁴ *Center for Severe Weather Research, Boulder, Colorado*

Accepted for publication on Feb. 12, 2015 in the
Bulletin of the American Meteorological Society

*Corresponding author address: Dept. of Atmospheric Sciences, University of Hawai‘i at Mānoa, 2525 Correa Rd., Honolulu, HI 96822

E-mail: mmbell@hawaii.edu

†Current affiliation: *Geophysical Fluid Dynamics Laboratory, Princeton, New Jersey*

3

CAPSULE

4 A Doppler on Wheels dual-polarimetric radar visited Hawai‘i for the first time on a National
5 Science Foundation Educational Deployment as part of a radar meteorology course at the
6 University of Hawai‘i at Mānoa.

7

8

ABSTRACT

9 A National Science Foundation sponsored Educational Deployment of a Doppler on Wheels
10 radar called the Hawaiian Educational Radar Opportunity (HERO) was conducted on O‘ahu
11 from 21 October to 13 November 2013. This was the first ever deployment of a dual-
12 polarimetric X-band (3-cm) research radar in Hawai‘i. A unique fine-resolution radar and
13 radiosonde dataset was collected during 16 intensive observing periods through a collabora-
14 tive effort between undergraduate and graduate students at University of Hawai‘i at Mānoa
15 and the Honolulu National Weather Service. HERO was the field component of MET 628
16 “Radar Meteorology”, with 12 enrolled graduate students who collected and analyzed the
17 data as part of the course. Extensive community outreach was conducted, including partici-
18 pation in a School of Ocean and Earth Science and Technology Open House event with over
19 7,500 visitors from local K-12 schools and the public. An overview of the HERO project and
20 highlights of the most interesting tropical rain and cloud observations are described. Phe-
21 nomena observed by the radar include cumulus clouds, trade wind showers, deep convective
22 thunderstorms, and a widespread heavy rain event associated with a cold frontal passage.
23 Detailed cloud and precipitation structures and their interactions with O‘ahu terrain, unique
24 dual-polarimetric signatures, and the implications for the dynamics and microphysics of trop-
25 ical convection are presented.

26 1. Introduction

27 The Hawaiian Islands experience frequent rain events, ranging from light trade wind
28 showers to heavy orographic and synoptically forced rainfall, with occasional extreme rainfall
29 from flash-flooding and tropical cyclones. O‘ahu is a relatively small island in the state with
30 a size of 71 x 48 km, but it has the highest population with nearly one million people. Despite
31 the small size, the island has significant mesoscale variability in rainfall due to the complex
32 terrain of the Ko‘olau and Wai‘anae mountains (Schroeder 1977; Chu et al. 2009; Van Nguyen
33 et al. 2010; Hartley and Chen 2010; Murphy and Businger 2010). Doppler radar is one of
34 the only meteorological tools available that can probe the three-dimensional precipitation
35 and wind structure of tropical clouds, showers, thunderstorms, and tropical cyclones with
36 adequate spatial and temporal resolution to observe this variability. There is no permanent
37 Doppler radar on O‘ahu, but the island has radar coverage from two Weather Surveillance
38 Doppler radars (WSR-88Ds) located on the neighbor islands of Kaua‘i and Moloka‘i.

39 The importance of radar technology to both research and operational weather forecasting
40 has continued to grow over the years, especially with recent advances in dual-polarimetric
41 technology (Herzegh and Jameson 1992), including the polarimetric upgrade of the WSR-
42 88Ds completed in Spring 2013 (Doviak et al. 2000). While radar observations are included
43 in many courses at the University of Hawai‘i at Mānoa (UHM), a dedicated course on the
44 principles and application of this technology was not available until Fall 2013 with the advent
45 of a graduate course called MET 628 “Radar Meteorology”. As part of the inaugural offering
46 of MET 628, a National Science Foundation (NSF) Educational Deployment of the Doppler
47 on Wheels (DOW, Wurman et al. 1997; Wurman 2001; Dixon et al. 2013) was requested in
48 order to maximize the educational value of the course. The HERO Educational Deployment
49 featured three main avenues to integrate the hands-on experience provided by the DOW
50 radar visit: 1) strong integration with MET 628 for graduate students, 2) field planning,
51 deployment, and forecast experience for graduate and undergraduate students, and 3) public
52 education and outreach.

53 Research radars have only rarely visited the Hawaiian islands due to the distance from
54 the mainland United States. The earliest research radar deployment is believed to be a
55 warm rain research project by the Illinois State Water Survey using two 3-cm radars near
56 Hilo on the island of Hawai‘i in the summer of 1965 (Semonin et al. 1967). The last NSF-
57 funded radar deployment to the islands used two 5-cm radars near Hilo in the summer
58 of 1990 for the Hawaiian Rainband Project (HaRP, Carbone et al. 1998). No research
59 weather radars have been deployed previously to O‘ahu to the authors’ knowledge. The
60 HERO deployment offered an opportunity to provide field and forecasting experience for
61 meteorology students, and allowed for broad exposure for the NSF facility to the public,
62 including non-major UHM students and local K-12 students. Native Hawaiians and Pacific
63 Islanders are underrepresented in the atmospheric sciences, and the chance to tour a high-
64 tech weather radar was an exciting experience for several thousand Hawai‘i residents.

65 The Moloka‘i WSR-88D radar is approximately 100 km from the center of O‘ahu, and
66 the Kaua‘i radar is approximately 175 km away. The distance from the WSR-88D radars
67 to O‘ahu limits the ability to observe precipitation below 1 km altitude and at sufficiently
68 high spatial resolution for some research purposes. Mobile DOW radars permit targeted de-
69 ployments close to weather phenomena of interest, resulting in much finer-scale observations
70 than can be obtained by more distant stationary radars. The DOW radars are managed
71 and operated by the Center for Severe Weather Research (CSWR), and have been used
72 in a wide variety of mesoscale meteorological studies, observing tornadoes (Wurman et al.
73 2012), hurricanes (Kosiba and Wurman 2014), winter precipitation (Schultz et al. 2002), and
74 other phenomena. DOWs have been used in several educational deployments on the U.S.
75 mainland¹ (Richardson et al. 2008; Toth et al. 2011). The ability to deploy a mobile 3-cm
76 wavelength radar allowed for unprecedented resolution of convective scale features around
77 O‘ahu, with radar gate spacing down to 15 meters. The approximately 3-week deployment

¹A complete list of NSF educational deployments and information on how to request NSF facilities for educational purposes can be found at <https://www.eol.ucar.edu/educational-deployments>.

78 from 21 October to 13 November 2013 coincided with an active weather period, yielding a
79 wide sampling of weather conditions. Phenomena observed by the radar include cumulus
80 clouds, trade wind showers, deep convective thunderstorms, and a widespread heavy rain
81 event associated with a cold frontal passage.

82 A key component of HERO was accurate forecasting of the weather conditions and tar-
83 geted precipitation forecasts. UHM is a unique institution that has both a graduate and
84 undergraduate Atmospheric Sciences program, and has the local National Weather Service
85 (NWS) Honolulu Weather Forecast Office collocated in the same building on campus. The
86 Central Pacific Hurricane Center is also collocated in the local NWS office. One of the high-
87 lights of HERO was the opportunity for students to improve their tropical forecasting skills
88 under the guidance of skilled NWS forecasters.

89 This article summarizes the HERO project and highlights some of the detailed cloud and
90 precipitation structures observed during the field experiment. The integration with MET
91 628 and other UHM education and outreach activities are described in Section 2. Selected
92 radar observations and analysis are presented in Section 3, including unique dual-polarimetric
93 signatures and their implications for the dynamics and microphysics of tropical convection.
94 Lessons learned during the deployment and concluding remarks are presented in Section 4.

95 **2. The HERO Educational Deployment**

96 *a. MET 628 Radar Meteorology*

97 MET 628 is a graduate level course at UHM to teach students the history, theory, hard-
98 ware, and practical use of radar for meteorological applications. Students developed skills
99 in understanding, interpreting, and using radar observations for meteorological research and
100 operational forecasting. The Educational Deployment provided a focal point for the inte-
101 gration of lectures, weekly labs, field work, and original research in the course. The twelve
102 MET 628 students enrolled in the course became principal investigators (PIs) for HERO,

103 and handled all radar operations and deployments under the advisement of the senior PIs
104 and CSWR staff. A list of course topics by week and the HERO start and end dates are
105 presented in Table 1.

106 The first 8 weeks of class were dedicated to foundational material designed to prepare
107 the students for the arrival of the DOW. Weekly radar labs were conducted for practical
108 experience performing radar calculations and using past DOW data in radar software such
109 as the Solo program (Bell et al. 2013). Once the DOW arrived the material shifted to
110 study topics relevant to the project. Course lectures continued during the HERO project,
111 with several guest lectures and departmental seminars on radar conducted during that time.
112 After the HERO project was over, additional course materials on specialized radar topics
113 were presented, and the students turned their attention to the exceptional dataset collected
114 for their final research papers and class presentations.

115 A wide variety of research topics were selected from the different Intensive Observing
116 Periods (IOPs), with some of the highlights presented in this paper. A list of the student
117 projects conducted as part of the course is shown in Table 2. The timing of the HERO
118 deployment during the middle part of the semester proved to be advantageous for both
119 weather and the course layout. Students had received enough of the radar fundamentals
120 to be prepared for the DOW operations, and had enough time at the end of the semester
121 to conduct preliminary analyses using a dataset they collected themselves. In contrast to
122 research presentations in most courses, the final presentations served as both a review of the
123 field experiment and as a culmination of the students' data collection and analysis efforts.

124 *b. Weather Forecasting*

125 A daily forecast briefing and operations meeting was conducted at 0900 LST (1900 UTC).
126 Four person forecast teams composed of 2 undergraduate and 2 graduate student volunteers
127 were organized prior to the project for 6-day shifts each. The 6-day shifts enabled continuity
128 and training in the forecasts without overburdening the students for the whole project. Each

¹²⁹ student team would prepare the weather forecast and briefing with advice and assistance from
¹³⁰ a local NWS forecaster. This arrangement worked very well, and both the student and NWS
¹³¹ forecasters spoke highly of the positive benefits of the collaboration.

¹³² Each daily meeting started with a 15-minute weather briefing for rainfall placement on
¹³³ or near O‘ahu during the next 48 hours, with an outlook for any potential major events
¹³⁴ out to approximately 5 days. After the weather briefing, a discussion on operations was
¹³⁵ conducted amongst the PIs, other students, and NWS personnel. Though the weather was
¹³⁶ often pleasant and mild during the project, the weather variability and forecast difficulties
¹³⁷ proved both enlightening and challenging. The timing of precipitation proved to be especially
¹³⁸ challenging due to mesoscale variability that was not well captured by numerical weather
¹³⁹ prediction models in our data sparse region. The ability to have real assets like the DOW
¹⁴⁰ to deploy added a significant value to the forecast discussions. Unlike typical classroom
¹⁴¹ exercises where there is a low penalty for an incorrect forecast, the decision to call for a real
¹⁴² mission at 4 am local time was not taken lightly by the students. The variety of observed
¹⁴³ weather ultimately turned out to be quite exceptional for the project period, and allowed
¹⁴⁴ for a good range of forecast conditions and testing of numerical model skill in Hawai‘i.

¹⁴⁵ 3. Public Education and Outreach

¹⁴⁶ Another key aspect of HERO was public education and outreach for the local residents of
¹⁴⁷ O‘ahu. Like most places on the U.S. mainland the weather is a common topic of conversation
¹⁴⁸ and plays an important role in daily life. Even though the tropical weather in Hawai‘i is
¹⁴⁹ usually benign, the conditions can change quickly at any time of the year due to the potential
¹⁵⁰ for flooding or severe weather. Hurricanes such as Iniki (1992) and recently Iselle and Ana
¹⁵¹ (2014), while uncommon in Hawai‘i, can cause significant damage to the islands. It was
¹⁵² valuable to showcase the DOW as an NSF facility and its role in improving our understanding
¹⁵³ of severe weather to the local K-12 students and their families.

154 The timing of the HERO project took advantage of a significant community outreach
155 event conducted on the UHM campus biennially. The School of Ocean and Earth Science
156 and Technology (SOEST) Open House consisted of a two-day Friday and Saturday event,
157 with the first day focusing on K-12 students, and the second day primarily for families and
158 the general public. An estimated 7,600 visitors attended the event, and due to the DOW's
159 central location the vast majority of the attendees were able to see the rotating radar antenna
160 as they walked through the Open House. A large fraction of those students, teachers, and
161 families toured the inside of the DOW as the monitors displayed data from previous tornado
162 and hurricane deployments. A photo from local media coverage of the event in the Honolulu
163 Star-Advertiser newspaper showing three students with one of the DOW scientists is shown
164 in Figure 1.

165 An additional outreach event was conducted during one of the IOPs for visiting students
166 from the Variety School of Hawai'i that educates children with learning disabilities, attention
167 deficit disorder, and autism. Middle school students and teachers visited the radar to ask
168 questions and help launch a weather balloon. The experience was great for the students,
169 and they built a "weather wall of thunder" with drawings and pictures at their school after
170 the event. It is hoped that the Open House, media coverage, and radar visits helped to
171 encourage some young students to consider careers in atmospheric science, geoscience, or
172 another science and technology field.

173 4. Field Operations

174 IOPs were targeted to be centered on 1800 or 0000 UTC (0800 or 1400 LST) for ap-
175 proximately 6 hours on station. Student teams were assigned on a rotating schedule based
176 on availability, such that all MET 628 participants had at least 3 IOPs with the DOW.
177 The student PIs were required to write a detailed mission summary after each IOP. Support
178 teams accompanied the truck in private vehicles to assist with radiosonde launches, and to

179 observe and learn the DOW radar operations. The support teams consisted of a combination
180 of volunteer undergraduate and graduate students and NWS personnel.

181 Seventeen sites around O‘ahu were identified to observe different types of weather con-
182 ditions as part of a course lab assignment on the effects of radar beam blockage by complex
183 terrain. These sites were then refined based on site surveys with CSWR personnel that
184 assessed height clearance for the DOW, ground clutter, and beam blockage. The final sites
185 used in the project are shown in Fig. 2. The radar was based on Sand Island at the UHM
186 SOEST Marine Center, but radar operations were limited there due to radio interference.
187 The primary area of operations was on the windward side of O‘ahu, with scientific interests
188 on trade wind showers, orographic forcing, and warm rain precipitation processes. The site
189 in the central valley near Wahiawa was used during the cold frontal passage, and on two
190 weak trade wind days when the sea breeze and inland convection were active.

191 Since operational soundings are only launched twice a day from the neighbor islands and
192 not on O‘ahu, 14 research radiosondes were launched by the HERO participants during the
193 IOPs. The research soundings provided thermodynamic context for the radar observations,
194 and were a critical component of the deployment. Weather balloon launches were the primary
195 responsibility of the support team participants, allowing them to contribute productively to
196 each IOP. Radiosonde data was sent in real time to the forecasters at the NWS, providing
197 valuable local information for the forecasters to aid in decision making and the issuance of
198 weather watches and warnings.

199 A combination of plan-position indicator (PPI) and range-height indicator (RHI) scans
200 were used to observe clouds and precipitation. A variety of different scan modes were used
201 depending on the desired range, velocity, and spatial resolution. A “playbook” in the Op-
202 erations Manual contained the different scan modes, with selection of the appropriate mode
203 guided by the PIs and CSWR staff during the project. However, the ultimate decision on
204 which mode to use, and the scanning angles used in the PPIs and RHIs, rested with the MET
205 628 students. The ability, and responsibility, to make choices about the scan strategy proved

206 to be a powerful teaching tool. Photographs of the students from two of the deployments are
207 shown in Fig. 3, and a summary of the IOPs is shown in Table 3. Highlights from selected
208 IOPs are discussed in the following sections.

209 *a. IOP 1: Kahalu‘u Wet Trade Wind Showers*

210 The forecast for the first IOP on 24 October was for a weak trade wind regime with little
211 synoptic forcing and lower than average boundary layer moisture. Chances for precipitation
212 were forecast to be best during the early morning and would most likely result from radi-
213 ational cooling at cloud top resulting in enhanced showers offshore, and land breeze trade
214 wind convergence and topographical forcing on the windward coast as showers came onshore.
215 The DOW was deployed to Kahalu‘u Regional Park on the windward coast. Upon arrival
216 there was a band of precipitation just offshore, with overcast skies along the windward coast.

217 Despite the marginal forecast for precipitation, showers developed and produced locally
218 heavy rain shortly after the radar’s arrival. The abundant echoes allowed for a time-mean
219 composite shown in Fig. 4 used to investigate orographic wind enhancements. Time-mean
220 radar reflectivity (Fig. 4a) reveals that shower activity was fairly widespread around the
221 radar, but had a clear maximum on the steep terrain of the Ko‘olau mountains. The time-
222 mean Doppler velocity in Fig. 4b shows the prevailing east-northeasterly flow associated with
223 trade winds, with cool colors indicating winds toward the radar and warm colors indicating
224 winds away from the radar. Single-Doppler analysis of the time-mean velocity (not shown)
225 indicates that the flow decelerated as it came onshore at low-levels, but accelerated above
226 the mountain top. The deceleration is believed to be due to a weak land-breeze circulation
227 in the early morning hours and increased friction over land. The surface wind direction
228 measured from the DOW at 10 m height showed westerly winds suggesting downslope flow
229 prior to sunrise, with a shift to weak easterly flow shortly after sunrise (not shown). The
230 enhancement in trade wind showers over the O‘ahu terrain at this time coincides with a
231 climatological peak in rainfall in the early morning, and is consistent with the hypothesis

232 that the morning rainfall maximum is due primarily to nocturnal cooling (Chen and Nash
233 1994; Van Nguyen et al. 2010).

234 *b. IOP 2: Wahiawa Sea-breeze Thunderstorms*

235 Surface high pressure over the main Hawaiian Islands was forecast for this IOP on 27
236 October, with a cold air mass aloft associated with a nearby upper level low. Southerly flow
237 over the island the day before had advected higher than normal boundary layer moisture
238 over the island, which along with the cold air aloft contributed to higher than normal in-
239 stability. Deep convection was expected to develop over the central valley of O‘ahu during
240 the afternoon due to a combination of sea breeze convergence and upslope flow in a light
241 synoptic flow pattern. The Wahiawa location was chosen as the deployment site based upon
242 the tendency for sea breeze convergence to incite convection in the island interior.

243 Towering cumulus accompanied by showers were already occurring at the site upon the
244 DOW’s arrival. During the late morning hours several cells of deep convection developed
245 near the radar site, with thunder being heard at the site by 2208 UTC. Thunder is a rare
246 occurrence in Hawai‘i, with audible thunderstorms occurring only 5 –10 times per year on
247 average over the islands (National Oceanic and Atmospheric Administration 1985). At 2211
248 UTC, outflow from the thunderstorm to the west of the radar reached the DOW wind
249 instruments, with a peak wind speed of 8.4 m s^{-1} . Short-lived ordinary-cell deep convection
250 continued to develop and dissipate over the valley and nearby mountains throughout the
251 afternoon.

252 Despite the weak synoptic forcing, this day produced the deepest convection of the HERO
253 project. RHI images of two convective towers are shown in Fig. 5. The echo top for the
254 convective cell seen in the top panels at 2206 UTC had a height of 8 km, well above the
255 freezing level of 4.5 km. The attenuation corrected radar reflectivity (Fig. 5a) shows a strong
256 echo exceeding 50 dBZ near 2 km altitude.² Below the rain echo, a surface echo from the

²Reflectivity and differential reflectivity were corrected using a specific differential phase power law fol-

257 Wai‘anae mountains can also be seen. The high dBZ rain shaft is accompanied by a moderate
258 differential reflectivity Z_{DR} around 3 dB that increases towards the surface (Fig. 5b). The
259 differential reflectivity measures the aspect ratio of the raindrops, with larger Z_{DR} values
260 representing larger, more oblate raindrops. Strong attenuation of the radar signal results in
261 a low signal-to-noise ratio and very noisy Z_{DR} on the back side of the convective cell relative
262 to the radar.

263 The specific differential phase K_{DP} shown in Fig. 5c is very large, exceeding 13 deg km^{-1} .
264 The K_{DP} variable measures the differential speed at which the horizontal and vertical radar
265 pulses travel through the storm, and is proportional to the concentration of medium and
266 large sized raindrops. The combination of high dBZ, high K_{DP} , and moderate Z_{DR} indicates
267 the presence of very heavy rain containing a large number of medium sized droplets, charac-
268 teristic of tropical precipitation. Derived rain rates using an X-band K_{DP} based algorithm
269 (Wang and Chandrasekar 2010) suggest peak rain rates aloft of more than 138 mm hr^{-1} .
270 While there is uncertainty in this rainfall estimate, intense rain rates on this order were gen-
271 erated in less than 30 minutes in the short-lived convective cells, resulting in street flooding
272 in Honolulu.

273 Another intense, tall echo extending to 12 km altitude was observed a few minutes later
274 at 2218 UTC (Fig. 5d). The reflectivity was highly attenuated, resulting in only a weak echo
275 on the back side of the cell and a possible three-body scattering signature. A “flare echo”
276 is evident beyond the region of heavy rain with larger drops indicated by Z_{DR} exceeding 4
277 dB (Fig. 5e). The flare is believed to be due to Mie scattering off the large drops towards
278 the ground, reflection back to the drops, and further scattering back to the radar resulting
279 in a longer travel time for the radar pulse. The flare is similar to a “hail spike” seen with
280 large hail in 10-cm radars (Zrnić 1987; Wilson and Reum 1988; Lemon 1998), but is caused
281 here by raindrops that are large compared to the 3-cm radar wavelength. The K_{DP} in the
282 heavy rain region is around 6 deg km^{-1} , suggesting a lower concentration of larger raindrops
following the procedure described in Chapter 7.4.1 of Bringi and Chandrasekar (2001).

283 compared to the previous cell.

284 Rotation was observed in some of the clouds on this day as well (Fig. 6). The velocity
285 dipole evident in Fig. 6a indicates a weak cyclonic circulation at 2 km altitude that was
286 visually confirmed by the HERO participants. While the conditions over O‘ahu are typically
287 not supportive of tornadoes, weak funnel clouds are often reported with deeper convection in
288 Hawai‘i, with an average of 20 funnels reported per year (National Oceanic and Atmospheric
289 Administration 1985). Although no funnel cloud was evident from this convective cell, the
290 rotational signature was confirmed by a Moloka‘i WSR-88D scan at the same altitude. The
291 impressive detail resolved by the DOW compared to the WSR-88D is notable however, and
292 emphasizes the importance of close range for resolving convective scale details with weather
293 radar. The ability to bring the DOW very close to the observed weather phenomena was a
294 critical aspect of data collection during HERO.

295 c. IOP 12: Wahiawa Cold Frontal Passage

296 The forecast for the IOP on 10 November was for heavy rain with increased instability
297 due to unseasonably cold air aloft. A cold front was approaching the islands from the north
298 and was expected to bring unsettled weather with the chance for thunderstorms. The timing
299 of the front was uncertain as a line of convection ahead of the front approached the islands
300 from the north. The DOW was deployed at the Wahiawa site for an extended overnight
301 deployment, with three separate teams operating the radar consecutively for approximately
302 8 hours each.

303 The precipitation on this day was characterized by widespread stratiform rain, with
304 the heaviest rain organized into bands punctuated by deeper convective updrafts. An RHI
305 through one of the convective cells at 0520 UTC is shown in Fig. 7a, with reflectivity ex-
306 ceeding 40 dBZ. Columns of high Z_{DR} and K_{DP} are evident in Fig. 7b and d, suggesting an
307 intense updraft associated with the cell (Kumjian et al. 2014). The updraft also distorted
308 the melting level, indicated by the bulging layer of low correlation coefficient ρ_{HV} associated

309 with the stronger echo (Fig. 7c). The low correlation coefficient is associated with mixed-
310 phase conditions, and the distortion suggests the presence of large amounts of supercooled
311 water being lofted above the freezing level in this region.

312 As that active convective cell decayed over the next 20 minutes, the convection organized
313 into a broad rain band of stratiform precipitation at 0539 UTC (Fig. 7e-h). The remnants of
314 the previous cell are evident to the left of the figure near the radar, with higher reflectivity
315 and a column of high Z_{DR} (Fig. 7f). The transition from snow to rain is apparent in the
316 increased reflectivity below the melting layer due to the increased backscatter of liquid versus
317 ice, although there is no strong “bright-band” in the dBZ field associated with the melting
318 precipitation. In contrast, the melting layer is quite evident as a thin band of high Z_{DR} and
319 low ρ_{HV} (Fig. 7g). The height of the melting layer decreased by approximately 700 meters
320 from 0508 to 0610 UTC, with a strengthening mixed-phase signal in the dual-polarimetric
321 variables, suggesting a weakening updraft and greater melting over time.

322 The K_{DP} signature shows a distinct maximum above the freezing level near the -12 to
323 -15° C temperature level (near 6 km altitude). This strong signature in K_{DP} but lack of
324 corresponding increase in dBZ suggests a high concentration of smaller ice crystals. This
325 signature has been identified as enhanced growth of dendritic ice crystals in stratiform pre-
326 cipitation in Colorado (Kennedy and Rutledge 2011) and Italy (Bechini et al. 2012), and is
327 well correlated with stronger surface precipitation below the high K_{DP} in these regions. The
328 presence of this signature in stratiform precipitation in Hawai‘i at a different altitude, but
329 similar temperature, is consistent with the interpretation of enhanced vapor deposition and
330 crystal growth near -15° C due to the difference in saturation vapor pressure over ice and
331 water. An enhancement of the low-level dBZ, Z_{DR} , and K_{DP} associated with heavier rain
332 below the high K_{DP} region is also consistent with this physical interpretation and the pre-
333 cipitation correlation found in previous studies. High K_{DP} values at the echo top in Figs. 7d
334 and h are associated with low signal-to-noise and may not be due to physical processes.

335 While the radar data provides valuable insight into the precipitation, the interpretation of

336 the radar imagery and physical processes depends on the local thermodynamic and kinematic
337 environment. A radiosonde was launched prior to frontal passage during a break in the
338 precipitation at 0955 UTC. The pre-frontal temperature sounding revealed a lack of typical
339 low-level inversion and the presence of very cold air aloft for Hawai'i in November (Fig. 8a).
340 The humidity profile revealed a very deep moist layer up to 250 hPa. The winds were
341 characterized by northeasterly flow at the surface, transitioning to weak winds in the middle
342 troposphere, and stronger westerly winds aloft.

343 The operations teams transitioned at 1200 UTC to continue the extended IOP. Over
344 the southern shores there was widespread precipitation which caused flood advisories to be
345 issued for much of the island. O'ahu was under a Flash Flood Watch and then Warning as
346 heavy rain showers stationed themselves over the southern and windward coasts. Eventually
347 the Mānoa Stream reached its flood stage during the IOP. Precipitation anchored to the
348 Ko'olau mountains resulted in the highest 24-hr rainfall totals, with a maximum of 228.9
349 mm in the Moanalua range.

350 The third team continued operations the next morning as the front passed the radar site.
351 A diffuse band of showers associated with weakening convergence along the cold front itself
352 were affecting the site during the midday and afternoon hours. A radiosonde was launched
353 successfully at 1801 UTC, despite strong winds during preparation. The mid-atmosphere
354 had dried considerably behind the front (Fig. 8b), and began to return to more typical trade
355 wind inversion and enhanced northeasterly surface flow. A general increase in northeasterly
356 winds were noted during this IOP, and a 13.2 m s^{-1} wind gust was recorded on the DOW
357 mast instrumentation at 2139 UTC. Strong westerly winds were observed aloft that were
358 associated with the upper level low.

359 *d. IOP 14: Kualoa Ranch Cumulus Clouds*

360 After the cold front had passed through on 10 November, dry cool weather set in on the
361 islands. The forecast for 12 November was for light trade winds with little moisture. Since

it was the last day of HERO, one last mission to Kualoa Ranch was conducted in hopes of catching some morning trade wind showers. High resolution observations of short-lived small cumulus clouds were obtained. Fig. 9a shows a photograph of one such cloud at sunrise just offshore of O‘ahu, approximately 4 km from the radar. A RHI through the cloud with 15 m radar gate spacing reveals a cauliflower-like structure, with columns of enhanced dBZ (Fig. 9b) and Z_{DR} (Fig. 9c). The highest reflectivity near 15 dBZ was found near cloud top, suggesting condensational droplet growth in the weak updraft. Conversely, the highest Z_{DR} was found near cloud base, suggesting evaporation of falling droplets and a resulting shift toward a larger median drop size (Kumjian and Ryzhkov 2010).

Low-level negative Doppler velocity (Fig. 9d) indicates light trade wind flow toward the radar at low-levels, with distinct turrets of radially outward flow aloft associated with updrafts at the growing cloud top. The spectrum width (Fig. 9e) shows near zero velocity variance at low-levels topped with increasing variance aloft exceeding 3 m s^{-1} . The dBZ, velocity, and spectrum width are consistent with the interpretation of small updrafts associated with small-scale turbulence and droplet growth at the top of the cloud. This high level of detail of a non-precipitating system could only be observed by the DOW, as the closest WSR-88D radar beam was too broad and high to adequately observe the cloud.

5. Summary and Lessons Learned

The HERO project was extremely successful. The deep integration with MET 628 “Radar Meteorology” contributed to both a successful course and educational deployment by giving students a true hands-on learning experience. The arrival of the DOW in the middle of the semester was an ideal time for maximizing both the pre-deployment learning and post-deployment analysis. Incorporating weather balloon launches into the project and having dedicated forecast teams helped to involve undergraduate students and NWS forecasters directly so that they were active participants in the project. The radiosondes also provided

387 valuable scientific information that helped improve the educational value of the radar data
388 collection. HERO was the first field project for the majority of the students, and the feedback
389 from all students has been very positive. A group photograph of most of the ~50 HERO
390 participants is shown in Fig. 10.

391 The close collaboration with the NWS proved to be an important part of the project
392 which contributed greatly to student forecasting skill and experience, and also provided data
393 for operational weather forecasts and warnings. The willingness of the NWS forecasters to
394 volunteer their time and expertise was greatly appreciated. Collaborative student and NWS
395 radiosonde launches and forecast discussions are continuing at UHM as a result of the HERO
396 project.

397 Capitalizing on the exceptional organization of the SOEST Open House helped the DOW
398 showcase be a very large public outreach event reaching over 7,500 people. In addition,
399 positive media coverage of the DOW also reached a large percentage of the local population.
400 The outreach and media coverage ended up being important for operating in public areas.
401 Most of the people who came by the DOW with positive comments had heard about the
402 radar from the media. A small percentage of people were confused or troubled by the radar's
403 presence around the island, with most of them changing their minds after talking with the
404 PI or UHM students.

405 Some of the difficulties operating on O'ahu were the lack of space in the congested urban
406 environment and steep and variable terrain. Unlike many mainland deployments where the
407 DOW can park and operate freely, the parking and deployment locations were strongly
408 constrained by available space, ground clutter, and terrain blocking. There were few side-
409 of-the-road spots where the DOW could operate, such that public parks were a primary
410 IOP option. Many public parks did not open early enough to operate during the nocturnal
411 convective maxima, therefore night-time operations were limited. Later in the day, the parks
412 became crowded with both locals and tourists who had mixed reactions to the radar and
413 associated generator noise. Privately owned locations identified during the project proved

⁴¹⁴ to be the best places to operate, and it is planned to more actively involve local landowners
⁴¹⁵ for any future DOW projects in Hawai‘i.

⁴¹⁶ Despite some of the difficulties with the urban environment, the meteorology on O‘ahu
⁴¹⁷ proved ideal for an educational deployment. The abundance of clouds and rain in the tropics
⁴¹⁸ helped to keep the project exciting for the entire duration, and there were a few uncommon
⁴¹⁹ events such as thunderstorms and a frontal passage. The detailed observations of early
⁴²⁰ morning trade wind showers suggest both nocturnal cooling and orographic effects played
⁴²¹ important roles in enhancing rainfall. Observations of deeper sea-breeze convection where
⁴²² heavy rainfall formed in a short period indicated variability in the drop size distribution,
⁴²³ with dual-polarimetric variables suggesting high concentrations of smaller raindrops and
⁴²⁴ lower concentrations of larger raindrops in different convective cells.

⁴²⁵ Coincident radiosondes and radar observations during cold frontal passage suggest the
⁴²⁶ presence of significant moisture and a pronounced melting level in stratiform precipitation
⁴²⁷ that was frequently distorted by convective updrafts. High specific differential phase mea-
⁴²⁸ surements above the melting level suggest enhanced growth of ice crystals near -15° C
⁴²⁹ leading to higher mesoscale rainfall amounts below these regions. High-resolution observa-
⁴³⁰ tions of non-precipitating cumulus clouds were also obtained, revealing weak reflectivity and
⁴³¹ differential reflectivity columns with multiple updrafts and turbulence at cloud top.

⁴³² In all of the above examples, coincident WSR-88D data was also recorded to provide
⁴³³ a valuable comparison of radar characteristics at the 10-cm wavelength, albeit at a much
⁴³⁴ coarser resolution than that obtained with the DOW. In some cases the phenomena were
⁴³⁵ only observed by the DOW due to the beam height and range of the WSR-88D, highlighting
⁴³⁶ the advantage of a mobile radar in the Hawaiian Islands. The fine-resolution 3-cm radar
⁴³⁷ observations of tropical weather in the central Pacific are novel and bear further study. An
⁴³⁸ exceptional dataset was collected during HERO, and valuable insights into tropical weather
⁴³⁹ and microphysical processes are expected upon further analysis. The data is freely available
⁴⁴⁰ to other interested researchers.

⁴⁴¹ *Acknowledgments.*

⁴⁴² The HERO project was supported by the National Science Foundation Lower Atmo-
⁴⁴³ spheric Observing Facilities, and the subsequent analysis and publication was supported
⁴⁴⁴ under NSF award AGS-1349881. The DOW Facility is supported by NSF award AGS-
⁴⁴⁵ 1361237. WCL's participation in the project was supported by the University Corporation
⁴⁴⁶ for Atmospheric Research UVISIT program. We thank all of the field project participants
⁴⁴⁷ who contributed to the project success, including Jeff Keeler, the UHM students, and NWS
⁴⁴⁸ personnel. Special thanks also go to David Morgan at Kualoa Ranch and the Waikalua Loko
⁴⁴⁹ Fishpond Board of Directors for the use of their property for data collection.

REFERENCES

- 452 Bechini, R., L. Baldini, and V. Chandrasekar, 2012: Polarimetric radar observations in the
 453 ice region of precipitating clouds at C-band and X-band radar frequencies. *J. Appl. Meteor.*
 454 *Climatol.*, **52** (5), 1147–1169, doi:10.1175/JAMC-D-12-055.1, URL <http://dx.doi.org/10.1175/JAMC-D-12-055.1>.
- 455
- 456 Bell, M. M., W.-C. Lee, C. A. Wolff, and H. Cai, 2013: A Solo-based automated qual-
 457 ity control algorithm for airborne tail Doppler radar data. *J. Appl. Meteor. Climati-
 458 tol.*, **52** (11), 2509–2528, doi:10.1175/JAMC-D-12-0283.1, URL <http://dx.doi.org/10.1175/JAMC-D-12-0283.1>.
- 459
- 460 Bringi, V. N. and V. Chandrasekar, 2001: *Polarimetric Doppler Weather Radar*. Cambridge
 461 University Press, 682 pp.
- 462 Carbone, R. E., J. D. Tuttle, W. A. Cooper, V. Grubišić, and W. C. Lee, 1998: Trade
 463 wind rainfall near the windward coast of Hawaii. *Mon. Wea. Rev.*, **126** (11), 2847–
 464 2863, doi:10.1175/1520-0493(1998)126<2847:TWRNTW>2.0.CO;2, URL [http://dx.doi.org/10.1175/1520-0493\(1998\)126<2847:TWRNTW>2.0.CO;2](http://dx.doi.org/10.1175/1520-0493(1998)126<2847:TWRNTW>2.0.CO;2).
- 465
- 466 Chen, Y.-L. and A. J. Nash, 1994: Diurnal variation of surface airflow and rain-
 467 fall frequencies on the island of Hawaii. *Mon. Wea. Rev.*, **122** (1), 34–56, doi:10.
 468 1175/1520-0493(1994)122<0034:DVOSAA>2.0.CO;2, URL [http://dx.doi.org/10.1175/1520-0493\(1994\)122<0034:DVOSAA>2.0.CO;2](http://dx.doi.org/10.1175/1520-0493(1994)122<0034:DVOSAA>2.0.CO;2).
- 469
- 470 Chu, P.-S., X. Zhao, Y. Ruan, and M. Grubbs, 2009: Extreme rainfall events in the Hawaiian
 471 islands. *J. Appl. Meteor. Climatol.*, **48** (3), 502–516, doi:10.1175/2008JAMC1829.1, URL
 472 <http://dx.doi.org/10.1175/2008JAMC1829.1>.

- 473 Dixon, M., E. Loew, J. Wurman, and K. Kosiba, 2013: Signal processing in the DOWs using
474 Pentek processors. *36th Conference on Radar Meteorology, Breckenridge, Colorado*, Amer.
475 Meteor. Soc.
- 476 Doviak, R. J., V. Bringi, A. Ryzhkov, A. Zahrai, and D. Zrnić, 2000: Considerations
477 for polarimetric upgrades to operational WSR-88D radars. *J. Atmos. Oceanic Tech-*
478 *nol.*, **17** (3), 257–278, doi:10.1175/1520-0426(2000)017<0257:CFPUTO>2.0.CO;2, URL
479 [http://dx.doi.org/10.1175/1520-0426\(2000\)017<0257:CFPUTO>2.0.CO;2](http://dx.doi.org/10.1175/1520-0426(2000)017<0257:CFPUTO>2.0.CO;2).
- 480 Hartley, T. M. and Y.-L. Chen, 2010: Characteristics of summer trade wind rainfall over
481 Oahu. *Wea. Forecasting*, **25** (6), 1797–1815, doi:10.1175/2010WAF2222328.1, URL <http://dx.doi.org/10.1175/2010WAF2222328.1>.
- 483 Herzegh, P. H. and A. R. Jameson, 1992: Observing precipitation through dual-
484 polarization radar measurements. *Bull. Amer. Meteor. Soc.*, **73** (9), 1365–1374, doi:10.
485 1175/1520-0477(1992)073<1365:OPTDPR>2.0.CO;2, URL [http://dx.doi.org/10.1175/1520-0477\(1992\)073<1365:OPTDPR>2.0.CO;2](http://dx.doi.org/10.1175/1520-0477(1992)073<1365:OPTDPR>2.0.CO;2).
- 487 Kennedy, P. C. and S. A. Rutledge, 2011: S-band dual-polarization radar observations of
488 winter storms. *J. Appl. Meteor. Climatol.*, **50**, 844–858, doi:10.1175/2010JAMC2558.1,
489 URL <http://dx.doi.org/10.1175/2010JAMC2558.1>.
- 490 Kosiba, K. A. and J. Wurman, 2014: Finescale dual-Doppler analysis of hurricane
491 boundary layer structures in Hurricane Frances (2004) at landfall. *Mon. Wea. Rev.*,
492 **142** (5), 1874–1891, doi:10.1175/MWR-D-13-00178.1, URL <http://dx.doi.org/10.1175/MWR-D-13-00178.1>.
- 494 Kumjian, M. R., A. P. Khain, N. Benmoshe, E. Ilotoviz, A. V. Ryzhkov, and V. T. J.
495 Phillips, 2014: The anatomy and physics of ZDR columns: Investigating a polarimet-
496 ric radar signature with a spectral bin microphysical model. *J. Appl. Meteor. Climatol.*,

- 497 **53** (7), 1820–1843, doi:10.1175/JAMC-D-13-0354.1, URL <http://dx.doi.org/10.1175/JAMC-D-13-0354.1>.
- 499 Kumjian, M. R. and A. V. Ryzhkov, 2010: The impact of evaporation on polarimetric
500 characteristics of rain: Theoretical model and practical implications. *J. Appl. Meteor.*
501 *Climatol.*, **49** (6), 1247–1267, doi:10.1175/2010JAMC2243.1, URL <http://dx.doi.org/10.1175/2010JAMC2243.1>.
- 503 Lemon, L. R., 1998: The radar “three-body scatter spike”: An operational large-hail signa-
504 ture. *Wea. Forecasting*, **13** (2), 327–340, doi:10.1175/1520-0434(1998)013<0327:TRTBSS>
505 2.0.CO;2, URL [http://dx.doi.org/10.1175/1520-0434\(1998\)013<0327:TRTBSS>2.0.CO;2](http://dx.doi.org/10.1175/1520-0434(1998)013<0327:TRTBSS>2.0.CO;2).
- 507 Murphy, M. J. and S. Businger, 2010: Orographic influences on an Oahu flood. *Mon. Wea.
508 Rev.*, **139** (7), 2198–2217, doi:10.1175/2010MWR3357.1, URL <http://dx.doi.org/10.1175/2010MWR3357.1>.
- 510 National Oceanic and Atmospheric Administration, 1985: *Narrative Summaries, Tables and
511 Maps for Each State with Overview of State Climatologist Programs*, Vol. 1: Alabama-New
512 Mexico. 3d ed., Gale Research Company, <http://www.wrcc.dri.edu/narratives/hawaii/>.
- 513 Richardson, Y., P. Markowski, J. Verlinde, and J. Wurman, 2008: FIELD EXPERI-
514 ENCE: Integrating classroom learning and research: The Pennsylvania Area Mobile
515 Radar Experiment (PAMREX). *Bull. Amer. Meteor. Soc.*, **89** (8), 1097–1101, doi:
516 10.1175/2007BAMS2567.1, URL <http://dx.doi.org/10.1175/2007BAMS2567.1>.
- 517 Schroeder, T. A., 1977: Meteorological analysis of an Oahu flood. *Mon. Wea. Rev.*, **105** (4),
518 458–468, doi:10.1175/1520-0493(1977)105<0458:MAOAOF>2.0.CO;2, URL [http://dx.doi.org/10.1175/1520-0493\(1977\)105<0458:MAOAOF>2.0.CO;2](http://dx.doi.org/10.1175/1520-0493(1977)105<0458:MAOAOF>2.0.CO;2).
- 520 Schultz, D. M., et al., 2002: Understanding Utah winter storms: The intermoun-
521 tain precipitation experiment. *Bull. Amer. Meteor. Soc.*, **83** (2), 189–210, doi:10.

- 522 1175/1520-0477(2002)083<0189:UUWSTI>2.3.CO;2, URL [http://dx.doi.org/10.1175/1520-0477\(2002\)083<0189:UUWSTI>2.3.CO;2](http://dx.doi.org/10.1175/1520-0477(2002)083<0189:UUWSTI>2.3.CO;2).
- 524 Semonin, R. G., E. A. Mueller, G. E. Stout, and D. W. Staggs, 1967: Radar analysis of
525 Project Warm Rain, Hilo, Hawaii-Summer 1965. ISWS Contract report CR-74, Illinois
526 State Water Survey, <http://hdl.handle.net/2142/55495>.
- 527 Toth, M., E. Jones, D. Pittman, and D. Solomon, 2011: DOW radar observations of wind
528 farms. *Bull. Amer. Meteor. Soc.*, **92** (8), 987–995, doi:10.1175/2011BAMS3068.1, URL
529 <http://dx.doi.org/10.1175/2011BAMS3068.1>.
- 530 Van Nguyen, H., Y.-L. Chen, and F. Fujioka, 2010: Numerical simulations of island effects
531 on airflow and weather during the summer over the island of Oahu. *Mon. Wea. Rev.*,
532 **138** (6), 2253–2280, doi:10.1175/2009MWR3203.1, URL <http://dx.doi.org/10.1175/2009MWR3203.1>.
- 534 Wang, Y. and V. Chandrasekar, 2010: Quantitative precipitation estimation in the CASA
535 X-band dual-polarization radar network. *J. Atmos. Oceanic Technol.*, **27** (10), 1665–1676,
536 doi:10.1175/2010JTECHA1419.1, URL <http://dx.doi.org/10.1175/2010JTECHA1419.1>.
- 537 1.
- 538 Wilson, J. W. and D. Reum, 1988: The flare echo: Reflectivity and velocity signature. *J. At-*
539 *mos. Oceanic Technol.*, **5** (2), 197–205, doi:10.1175/1520-0426(1988)005<0197:TFERAV>
540 2.0.CO;2, URL [http://dx.doi.org/10.1175/1520-0426\(1988\)005<0197:TFERAV>2.0.CO;2](http://dx.doi.org/10.1175/1520-0426(1988)005<0197:TFERAV>2.0.CO;2).
- 542 Wurman, J., 2001: The DOW mobile multiple Doppler network. *30th International Confer-*
543 *ence on Radar Meteorology, Munich, Germany*, Amer. Meteor. Soc., 95–97.
- 544 Wurman, J., D. Dowell, Y. Richardson, P. Markowski, E. Rasmussen, D. Burgess, L. Wicker,
545 and H. B. Bluestein, 2012: The second Verification of the Origins of Rotation in Tor-

- 546 nadoes Experiment: VORTEX2. *Bull. Amer. Meteor. Soc.*, **93** (8), 1147–1170, doi:
547 10.1175/BAMS-D-11-00010.1, URL <http://dx.doi.org/10.1175/BAMS-D-11-00010.1>.
- 548 Wurman, J., J. Straka, E. Rasmussen, M. Randall, and A. Zahrai, 1997: Design and de-
549 ployment of a portable, pencil-beam, pulsed, 3-cm Doppler radar. *J. Atmos. Oceanic
550 Technol.*, **14** (6), 1502–1512, doi:10.1175/1520-0426(1997)014<1502:DADOAP>2.0.CO;2,
551 URL [http://dx.doi.org/10.1175/1520-0426\(1997\)014<1502:DADOAP>2.0.CO;2](http://dx.doi.org/10.1175/1520-0426(1997)014<1502:DADOAP>2.0.CO;2).
- 552 Zrnić, D. S., 1987: Three-body scattering produces precipitation signature of special diag-
553 nostic value. *Radio Science*, **22** (1), 76–86, doi:10.1029/RS022i001p00076, URL <http://dx.doi.org/10.1029/RS022i001p00076>.
- 554

555 **List of Tables**

<small>556</small>	1	MET 628 radar topics and HERO schedule	25
<small>557</small>	2	List of Student Research Projects from HERO	26
<small>558</small>	3	Summary of HERO Intensive Observing Periods	27

TABLE 1. MET 628 radar topics and HERO schedule

<i>Week</i>	<i>MET 628 Course Topic</i>
1	Introduction to weather radar hardware and technology
2	Polarimetric electromagnetic wave propagation and scattering
3	Radar equation derivation and analysis for point targets
4	36th AMS Conference on Radar Meteorology
5	Radar equation for distributed targets
6	Radar moment estimation
7	Dual-polarimetric radar variables
8	Precipitation estimation and particle identification
9	Mobile radars
	DOW Arrives for HERO on 21 October
10	Single-Doppler wind retrieval techniques
11	Multi-Doppler wind retrieval techniques
12	Severe weather applications
	HERO concludes on 13 November
13	Clear-air applications including wind profilers
14	Advanced signal processing
15	Radar data assimilation techniques
16	Advanced and future radar technologies
17	Final class presentations

TABLE 2. List of Student Research Projects from HERO

<i>Author</i>	<i>IOP Used</i>	<i>Project Title</i>
Almanza, V.	12	Dual-Doppler Analysis During a Subtropical Rainfall Event
Bauman, M.	12	Comparing Mobile Doppler Radar Characteristics of Convective and Stratiform Regions of a Tropical Line of Convection
Ballard, R.	2, 10	Mobile Polarimetric Radar Observations of Sea Breeze Convection on Oahu
Foerster, A.	1	Trade Wind Flow Interaction with the Ko'olaus
Frambach, A.	2	Hydrometeor Classification in Hawaii Using the DOW7 X-Band Dual-Polarization Mobile Radar During the HERO Project
Grunseich, G.	4, 5,10	Validation of Doppler Velocities gathered during the Hawaiian Educational Radar Opportunity (HERO) under different weather regimes
Hsiao, F.	12	Assimilation of Radar data with SAMURAI for a Cold Front Case in Oahu, Hawaii
Li, L.	12	Z-R Relationship for Cold Frontal Precipitation in Hawaii
Pattantyus, A.	5	Tropical Squall Line Features and Characteristics Observed with the Doppler on Wheels during the Hawaii Educational Radar Opportunity
Rees, S.	14	Solar Calibration and Antenna Patterns of the DOW 7
Robinson, T.	4	Radar Validation of Orographic Shape Vertical Motion Model
Sockol, A.	12	A Statistical Analysis of the November 10th, 2013 Storm on the Island of Oahu

TABLE 3. Summary of HERO Intensive Observing Periods

IOP #	Date	Start	End (UTC)	Event
1	24 Oct.	1510	2040	Kahalu'u Wet Trade Wind Showers
2	27 Oct.	1952	0130	Wahiawa Sea-breeze Thunderstorms
3	29 Oct.	1514	2017	Kahalu'u Weak Trade Wind Showers
4	30 Oct.	1824	2255	Fishpond Moderate Trade Wind Showers
5	31 Oct.	1519	2228	Kahalu'u Tropical Squall Line
6	1 Nov.	1513	2011	Makapu'u Offshore Trade Wind Showers
7	3 Nov.	1514	2017	Kahalu'u Orographic Showers
8	4 Nov.	1550	2204	Kahalu'u Cold Air Aloft
9	5 Nov.	1521	1818	Pali Lookout Weak Trade Winds
10	7 Nov.	2000	0200	Wahiawa Sea-breeze Convection
11	8 Nov.	1527	2116	Kualoa Ranch Weak Trade Winds
12a	10 Nov.	0400	1200	Wahiawa Cold Frontal Passage "A"
12b	10 Nov.	1200	1949	Wahiawa Cold Frontal Passage "B"
12c	10 Nov.	1949	0153	Wahiawa Cold Frontal Passage "C"
13	12 Nov.	1615	2119	Mānoa Valley Post-frontal
14	13 Nov.	1535	1803	Kualoa Ranch Cumulus Clouds

559 **List of Figures**

560 1	Wai‘alae Elementary Public Charter School students Mandy Williams, left, 561 Kaiona Orr and Christen Horita chatted with research scientist Karen Kosiba 562 from CSWR about the Doppler on Wheels radar truck. Photo reprinted 563 courtesy of Craig Kojima / Honolulu Star-Advertiser.	30
564 2	Satellite image of O‘ahu showing radar sites used during the HERO project. 565 Image courtesy Google Earth.	31
566 3	HERO participants in the field with the DOW radar. (a) Kualoa Ranch during 567 IOP 14, (b) Waikalua Loko fishpond during IOP 4, (c) Kahalu‘u site during 568 IOP 1, and (d) sounding launch at Kualoa Ranch during IOP 11.	32
569 4	Temporal averages from 1658:09 to 1934:27 UTC on 24 October of (a) radar 570 reflectivity in dBZ and (b) Doppler velocity in m s^{-1} . The DOW is indi- 571 cated by the radar truck symbol, the O‘ahu coastline is denoted by the thick 572 blue line, and terrain contours every 250 m are denoted by black lines. The 573 750 m contour representing the approximately average height of the Ko‘olau 574 mountain range is highlighted by the thick black contour. The radar data was 575 averaged in polar coordinates on the 14° PPI elevation surface, then mapped 576 to a Mercator projection for comparison with the terrain.	33
577 5	RHI radar images on 27 October at 2206:55 UTC (top) and 2218:38 UTC 578 (bottom). (a, d) Radar reflectivity (dBZ), (b, e) differential reflectivity Z_{DR} 579 (dB), and (c, f) specific differential phase K_{DP} (deg km^{-1}). Tick marks denote 580 2 km in the vertical, and 10 km in the horizontal. The radar is at the bottom 581 left corner of each panel, and the RHIs are at 270° relative to the truck (224° 582 heading) at 2206 UTC, and 250° (204° heading) at 2218 UTC.	34

- 583 6 Doppler velocity in m s^{-1} on 27 October from (a) the DOW radar at 8.5°
584 elevation at 2324:31 UTC with the radar location indicated by the truck sym-
585 bol, and (b) WSR-88D Moloka'i radar at 0.5° elevation at 2318:48 UTC. The
586 rotation signature at 2.1 km height is highlighted by the circles, and arrows
587 indicate the direction and distance to the radar. Tick marks denote 5 km in
588 the horizontal. 35

589 7 RHI radar images on 10 November at 0520:25 (left) and 0539:41 UTC (right).
590 (a, e) Radar reflectivity (dBZ), (b, f) differential reflectivity Z_{DR} (dB), (c,
591 g) correlation coefficient ρ_{HV} , and (d, h) specific differential phase K_{DP} (deg
592 km^{-1}). Tick marks denote 2 km in the vertical, and 10 km in the horizontal.
593 The radar is at the bottom left corner of each panel, and the RHIs are at 240°
594 relative to the truck (108° heading). 36

595 8 Soundings launched on 10 November at (a) 0955 UTC and (b) 1801 UTC.
596 The ordinate is log of pressure (hPa) and the abscissa is skewed Temperature
597 ($^\circ\text{C}$). The red line denotes air temperature, the blue line denotes dew point
598 temperature, and wind barbs denote wind direction and speed in knots. 37

599 9 Cumulus cloud observations on 13 November. (a) Photo of the cloud at 1655
600 UTC, (b) radar reflectivity (dBZ), (c) differential reflectivity Z_{DR} (dB), (d)
601 Doppler velocity (m s^{-1}), and (e) spectrum width (m s^{-1}). Tick marks denote
602 1 km in the vertical and in the horizontal. The radar is at the bottom left
603 corner of each panel, and the RHIs are at 92° relative to the truck (57° heading). 38

604 10 HERO participants in front of the DOW on the UHM campus. The “shaka”
605 hand symbol seen in this and other photos is a well-known gesture used fre-
606 quently throughout Hawai'i to convey thanks, friendship, camaraderie, and
607 the Aloha spirit. 39



FIG. 1. Wai‘alae Elementary Public Charter School students Mandy Williams, left, Kaiona Orr and Christen Horita chatted with research scientist Karen Kosiba from CSWR about the Doppler on Wheels radar truck. Photo reprinted courtesy of Craig Kojima / Honolulu Star-Advertiser.



FIG. 2. Satellite image of O'ahu showing radar sites used during the HERO project. Image courtesy Google Earth.

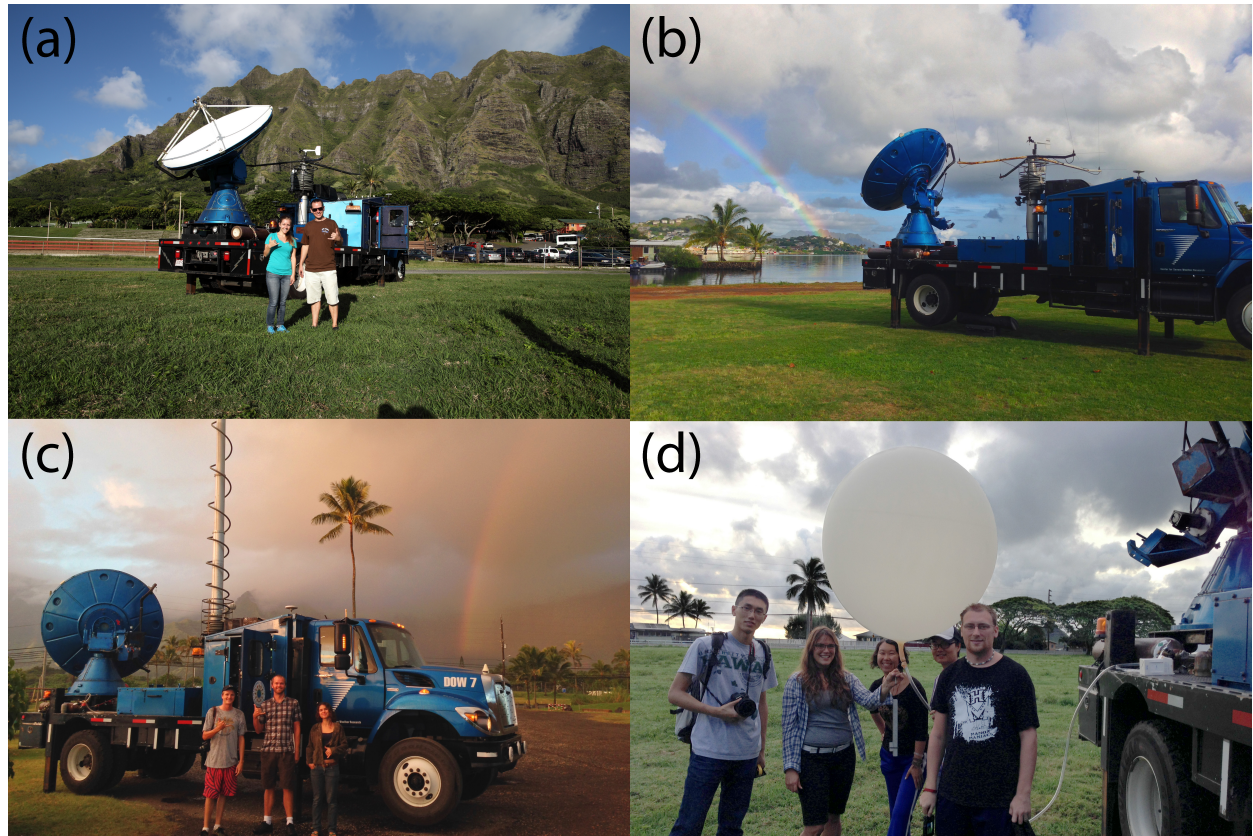


FIG. 3. HERO participants in the field with the DOW radar. (a) Kualoa Ranch during IOP 14, (b) Waikalua Loko fishpond during IOP 4, (c) Kahalu'u site during IOP 1, and (d) sounding launch at Kualoa Ranch during IOP 11.

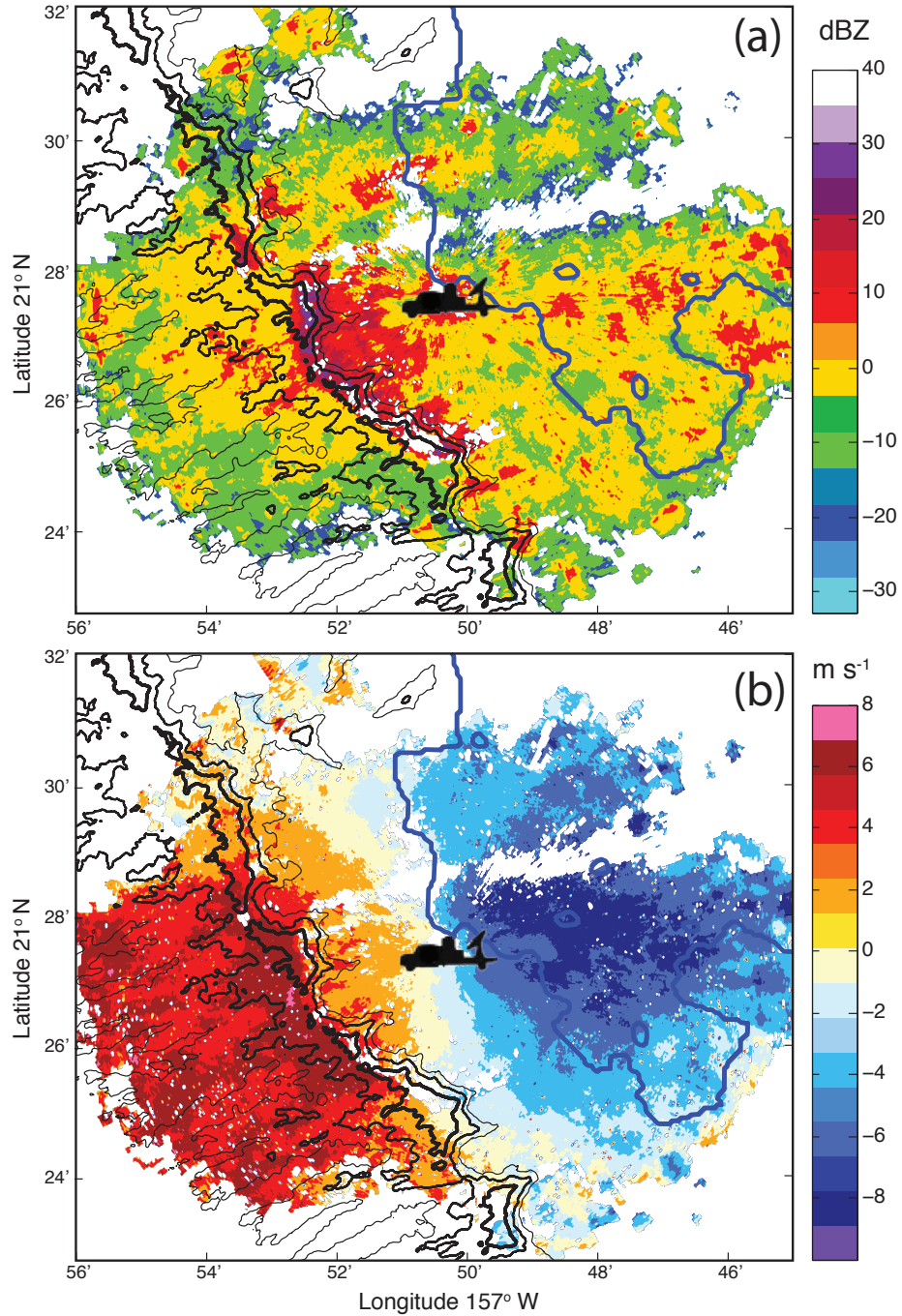


FIG. 4. Temporal averages from 1658:09 to 1934:27 UTC on 24 October of (a) radar reflectivity in dBZ and (b) Doppler velocity in m s^{-1} . The DOW is indicated by the radar truck symbol, the O'ahu coastline is denoted by the thick blue line, and terrain contours every 250 m are denoted by black lines. The 750 m contour representing the approximately average height of the Ko'olau mountain range is highlighted by the thick black contour. The radar data was averaged in polar coordinates on the 14° PPI elevation surface, then mapped to a Mercator projection for comparison with the terrain.

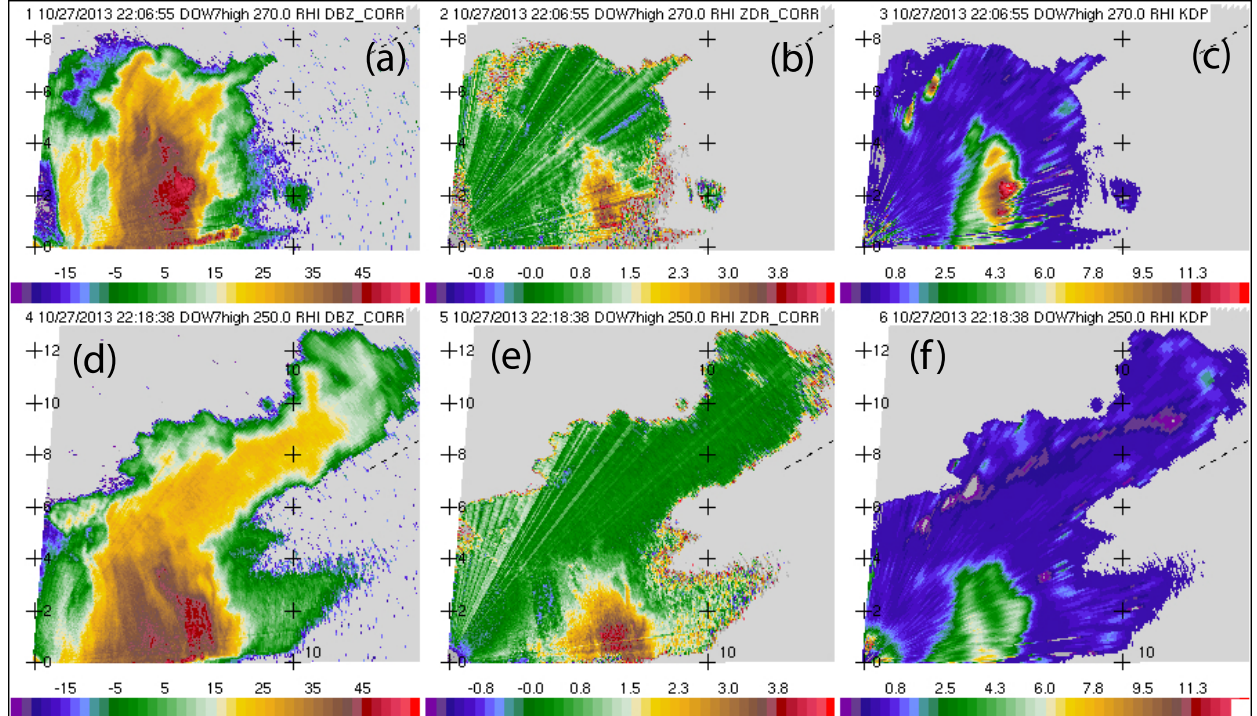


FIG. 5. RHI radar images on 27 October at 2206:55 UTC (top) and 2218:38 UTC (bottom). (a, d) Radar reflectivity (dBZ), (b, e) differential reflectivity Z_{DR} (dB), and (c, f) specific differential phase K_{DP} (deg km^{-1}). Tick marks denote 2 km in the vertical, and 10 km in the horizontal. The radar is at the bottom left corner of each panel, and the RHIs are at 270° relative to the truck (224° heading) at 2206 UTC, and 250° (204° heading) at 2218 UTC.

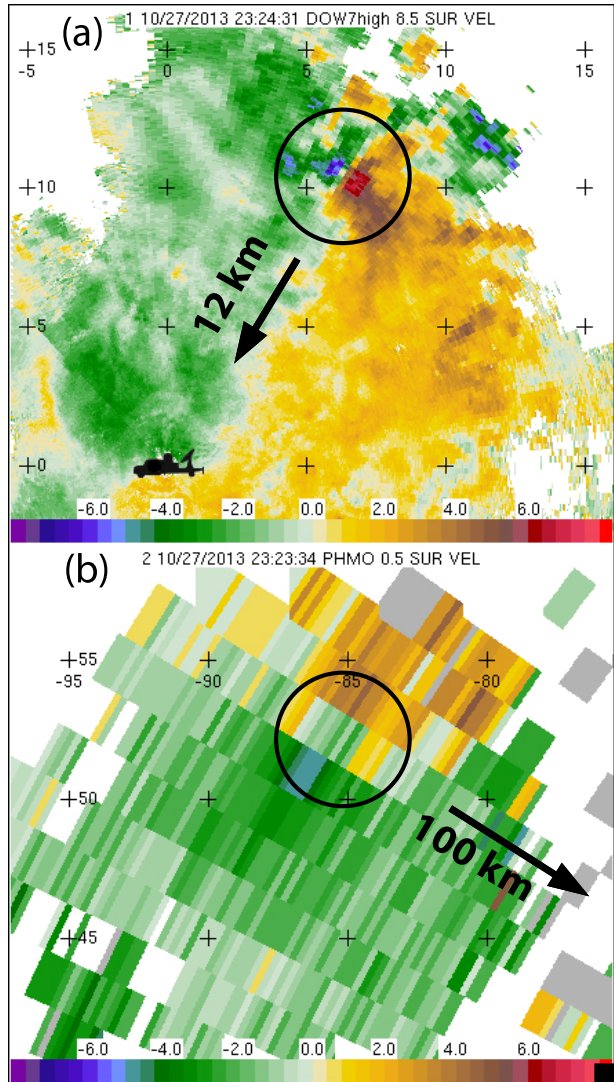


FIG. 6. Doppler velocity in m s^{-1} on 27 October from (a) the DOW radar at 8.5° elevation at 2324:31 UTC with the radar location indicated by the truck symbol, and (b) WSR-88D Molokai radar at 0.5° elevation at 2318:48 UTC. The rotation signature at 2.1 km height is highlighted by the circles, and arrows indicate the direction and distance to the radar. Tick marks denote 5 km in the horizontal.

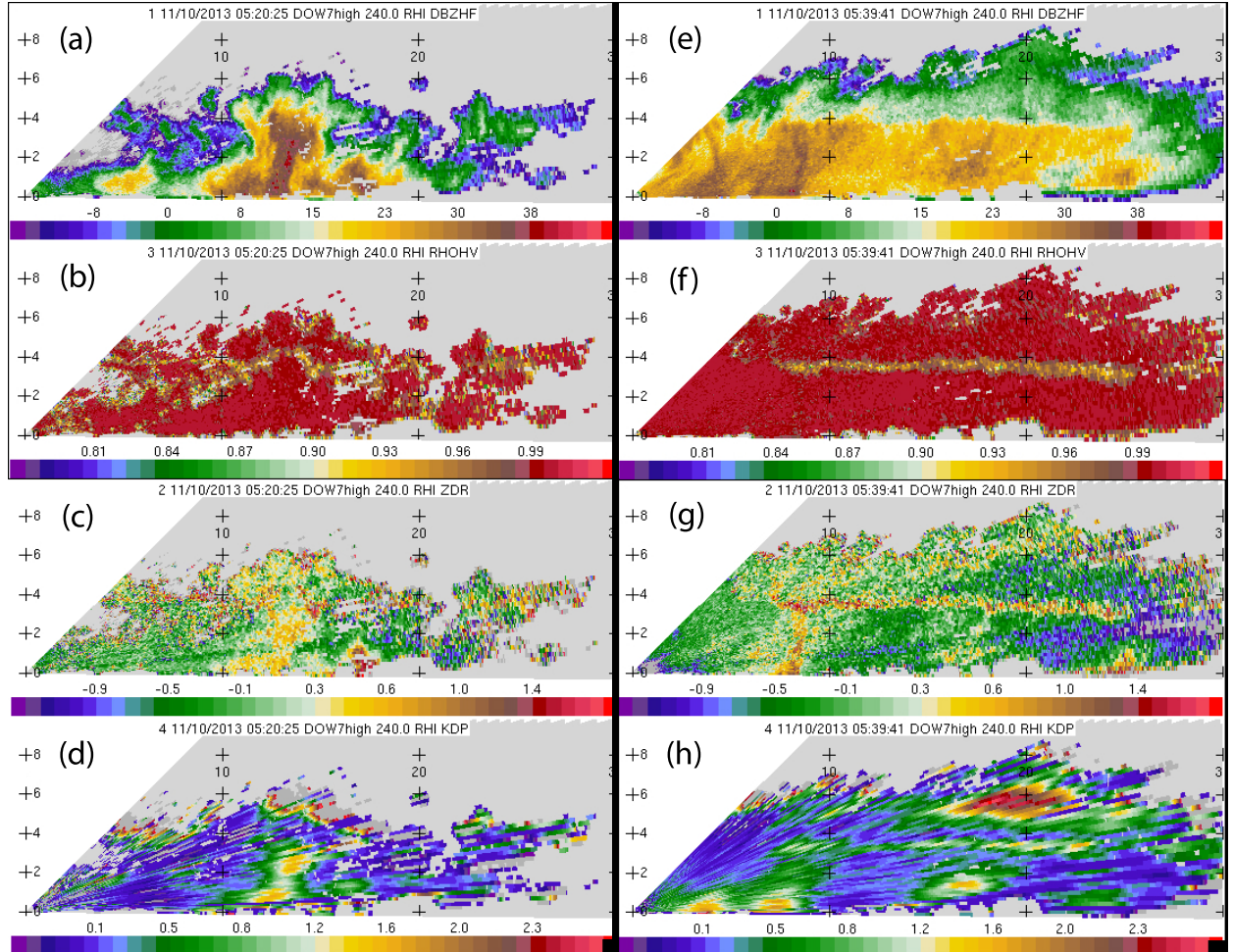


FIG. 7. RHI radar images on 10 November at 0520:25 (left) and 0539:41 UTC (right). (a, e) Radar reflectivity (dBZ), (b, f) differential reflectivity Z_{DR} (dB), (c, g) correlation coefficient ρ_{HV} , and (d, h) specific differential phase K_{DP} (deg km^{-1}). Tick marks denote 2 km in the vertical, and 10 km in the horizontal. The radar is at the bottom left corner of each panel, and the RHIs are at 240° relative to the truck (108° heading).

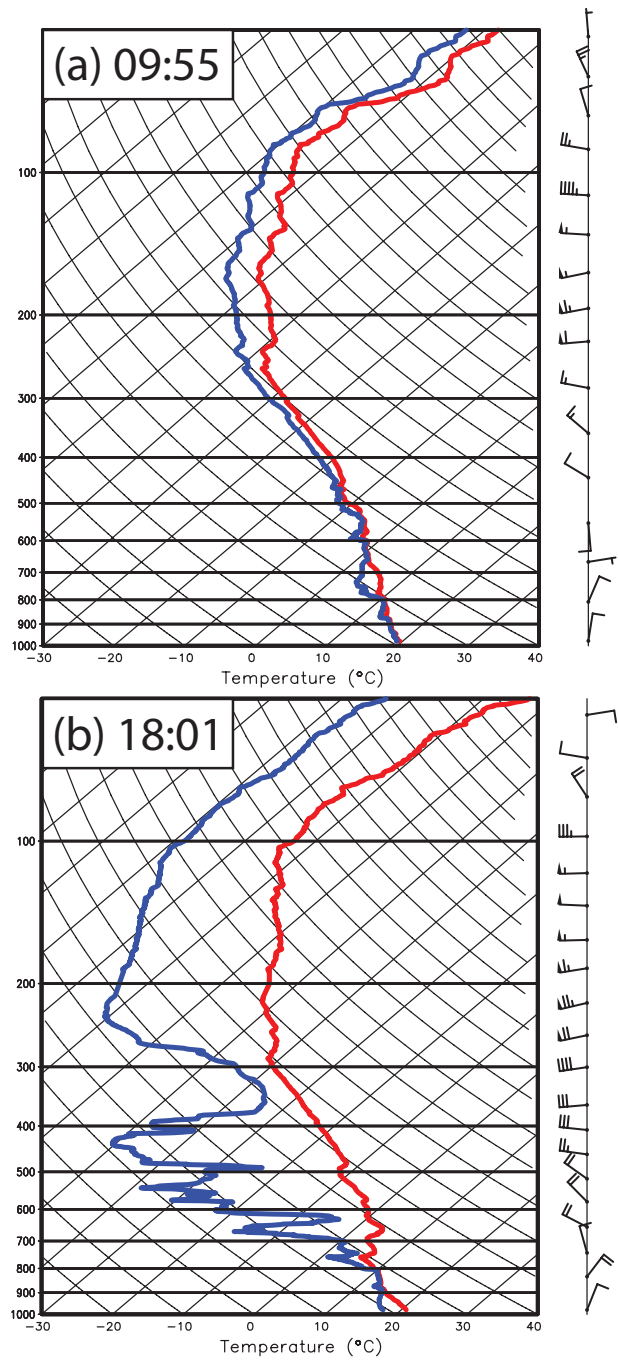


FIG. 8. Soundings launched on 10 November at (a) 0955 UTC and (b) 1801 UTC. The ordinate is log of pressure (hPa) and the abscissa is skewed Temperature ($^{\circ}\text{C}$). The red line denotes air temperature, the blue line denotes dew point temperature, and wind barbs denote wind direction and speed in knots.

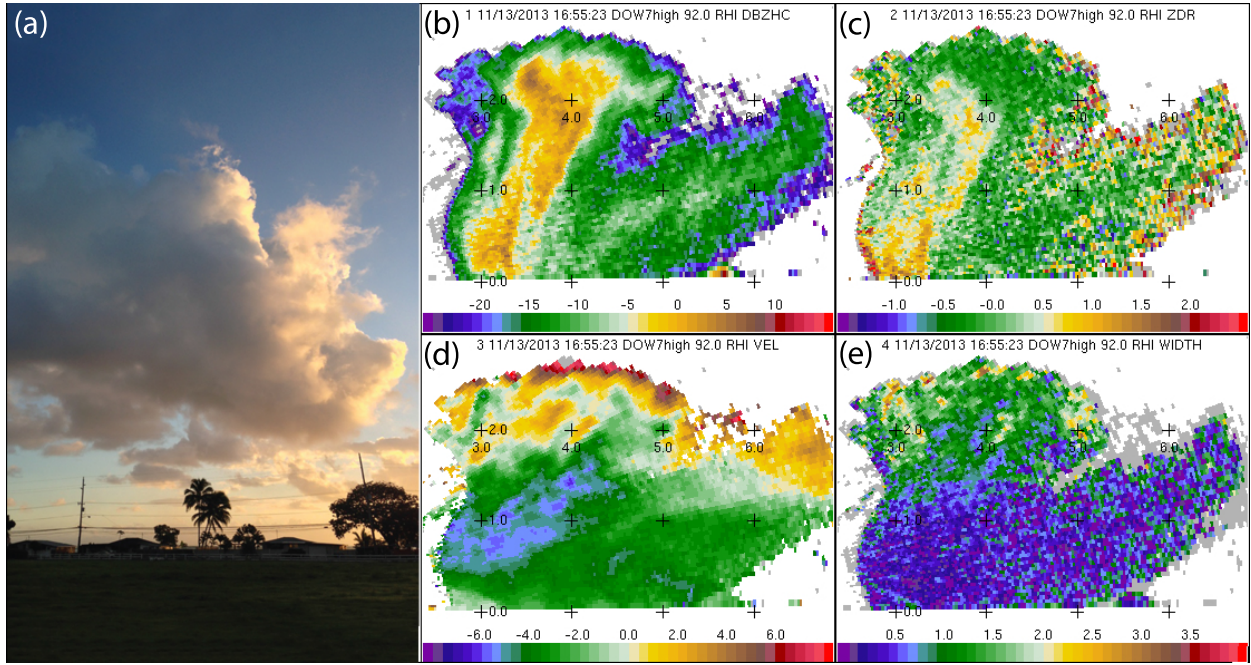


FIG. 9. Cumulus cloud observations on 13 November. (a) Photo of the cloud at 1655 UTC, (b) radar reflectivity (dBZ), (c) differential reflectivity Z_{DR} (dB), (d) Doppler velocity (m s^{-1}), and (e) spectrum width (m s^{-1}). Tick marks denote 1 km in the vertical and in the horizontal. The radar is at the bottom left corner of each panel, and the RHIs are at 92° relative to the truck (57° heading).



FIG. 10. HERO participants in front of the DOW on the UHM campus. The “shaka” hand symbol seen in this and other photos is a well-known gesture used frequently throughout Hawai‘i to convey thanks, friendship, camaraderie, and the Aloha spirit.